Communication

Regimes of Micro-bubble Formation Using Gas Injection into Ladle Shroud

SHENG CHANG, XIANGKUN CAO, and ZONGSHU ZOU

Gas injection into a ladle shroud is a practical approach to produce micro-bubbles in tundishes, to promote inclusion removal from liquid steel. A semi-empirical model was established to characterize the bubble formation considering the effect of shearing action combined with the non-fully bubble break-up by turbulence. The model shows a good accuracy in predicting the size of bubbles formed in complex flow within the ladle shroud.

https://doi.org/10.1007/s11663-018-1231-x

In tundish operations, Gas bubbling[1–4] is an effective methodology to enhance the removal of inclusions, especially for those smaller than 50 μm. The inclusion removal by bubble flotation occurs by two phenomena: adherence of inclusion on the bubble surface[5] and inclusion capture by the bubbles' wakes.[6] Furthermore, the upward flow caused by bubble flotation can also reduce the thermal stratification of liquid steel. Zhang and Taniguchi[7] reviewed the fundamentals of inclusions removal by gas bubbling. The probability of attachment and detachment between inclusions and bubbles was discussed on the basis of theories from particle flotation in mineral processing. They reported that small bubbles performed better in the removal of inclusions, owing to their high attachment probability for inclusions, long residence time, and large surface-to-volume ratio. Moreover, small bubbles are beneficial for maintaining a stable slag layer during gas blowing, which prevents heat loss and re-oxidization of liquid steel. Hence, minimizing the bubble size has been the focus of gas bubbling in tundish.

At present, gas curtain technique is commonly used to produce bubbles in tundish operations, in which gas was blown through a porous plug, forming a bubble column. Many studies had already successfully obtained bubbles around 2 mm (or even smaller) in water modeling, through decreasing gas flow rate and reducing the size of gas ports. Irons and Guthrie[8] performed experimental work to investigate the bubble formation in liquid pig iron at 1523 K. Bubble sizes were calculated by the bubble formation frequency combined with the gas flow rate. According to their results, the smallest bubbles, formed by a very small nozzle (1.6 mm) with an extremely low gas flow rate (0.03 L/min), were around 16 mm in diameter, which were still much bigger than the bubbles obtained in water modeling.

In the gas curtain technique, the porous plug was located at the bottom of tundish where the liquid flow was very slow and smooth, providing a quasi-static condition for bubble formation. The impact of liquid flow on bubble departure can be neglected. Since liquid steel has approximately 22 times higher surface tension and 7 times higher density than water, bubbles in liquid steel would bear a much higher capillary pressure (caused by the surface tension) and hydrostatic pressure (caused by gravity of the liquid) than those in water modeling. These pressures, acting on the gas liquid interface, prevent the bubble release and prolong the time of bubble growth based on gas ports, leading to an increase of gas quantity in the bubble. Furthermore, in actual tundish operation, the refractory porous plug was non-wetted with liquid steel, so that the bubble tends to spread along the port face, rather than being constrained to the diameter of the port. Even worse, this may result in the coalescence of bubbles from neighboring ports of the porous plug as shown in Figure 1, which will sharply increase the final size of bubbles. Therefore, based on both experimental study and theoretical analysis, it can be concluded that current gas curtain technique cannot produce micro-bubbles in liquid steel.

By contrast, gas injection into ladle shroud is a better methodology to make smaller bubbles in the tundish. Gas, released from the port on the inner wall of ladle shroud, is firstly sheared by high-speed inflow liquid, forming the original bubbles. And then, these bubbles are further refined by the turbulence within the flow system, which can effectively reduce the bubble size to micrometer scale.[9] In this approach, the liquid flow in ladle shroud dominated the process of bubble formation, by contrast, the impact of surface tension and interfacial wettability is much reduced. It is well known that the flow behavior of liquid steel is similar with that in its corresponding water modeling,[10] owing to the comparable kinematic viscosities between water and liquid steel. This improves the likelihood that the

SHENG CHANG is with the School of Metallurgy, Northeastern University, Shenyang, 110819, Liaoning, P.R. China and also with the McGill Metals Processing Centre, McGill University, Montreal, QC, H3A 2B2, Canada. Contact e-mail: chang.sheng@mail.mcgill.ca XIANGKUN CAO is with the McGill Metals Processing Centre, McGill University and also with the Sibley School of Mechanical and Aerospace Engineering, Cornell University, Ithaca, New York 14853. ZONGSHU ZOU is with the School of Metallurgy, Northeastern University.

Manuscript submitted July 31, 2017.
Article published online March 13, 2018.

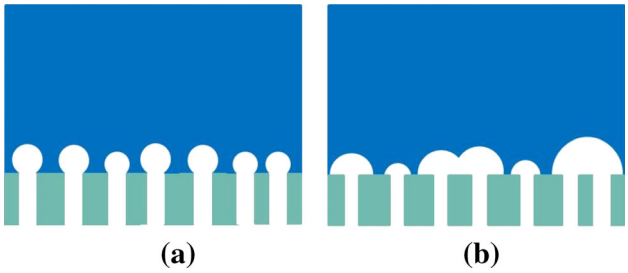

Fig. 1—Comparison of bubbles generated from (*a*) wetting and (*b*) non-wetting porous plugs.

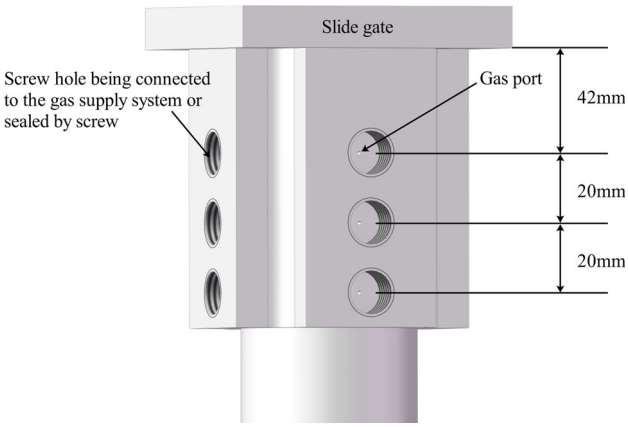

Fig. 2—The upper section of the novel ladle shroud with key dimensions (mm).

bubbles' size will be similar in water modeling and actual liquid steel for the same flow system. Hence, water modeling is a valid method to simulate the formation of bubbles in liquid steel, when using gas injection into ladle shroud.

A full-scaled water model was established based on a delta-shaped, four-strand prototype tundish with a novel shroud for gas blowing. As shown in Figure 2, bubbles were generated from laser-drilled gas injection ports (0.3 mm in diameter), located at the upper section of the shroud. These ports were uniformly distributed on three layers, 42, 62, and 82 mm beneath the slide gate, respectively. In terms of bubble record, a novel photography was developed to avoid the optical illusion effects caused by the distance between the bubble and lens from viewing bubbles on a 2-D plane. The setup of bubble measurement consists of an inclined plexiglass plate (with a 15 deg angle to the vertical), two pieces of LED light sheet, a high-speed camera, and a prime lens. The photo was post-processed by an open-source software, Image J, in order to obtain the average size of bubbles in each case. Detailed operation parameters of water modeling and bubble measurement could be found in a previous article.[11]

Figure 3 is a typical photo of bubbles formed using a port located at 42 mm below the slide gate, with a gas flow rate of 0.8 L/min. It is obvious that, most of the

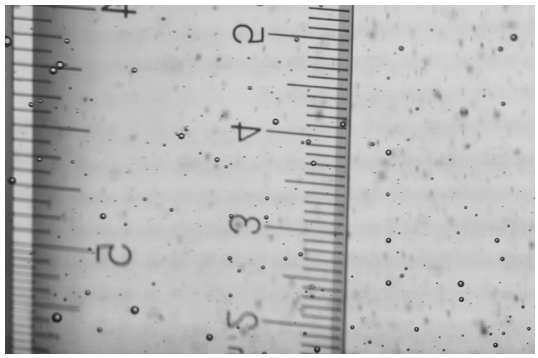

Fig. 3—A typical photo of bubbles generated using ladle shroud, compared with a scale.

Table I. Size of Bubbles Formed Under Various Gas Injection Schemes

Case	Gas Injection Position	Gas Flow Rate (L/min)	Bubble Size (μm)
1	1st layer	0.1	675
2		0.2	815
3		0.4	965
4		0.8	1117
5	2nd layer	0.1	743
6		0.2	895
7		0.4	1132
8		0.8	1380
9	3rd layer	0.1	764
10		0.2	915
11		0.4	1287
12		0.8	1664

bubbles are smaller than 1 mm, owing to the usage of the novel ladle shroud. As such, they can be defined as micro-bubbles. In order to clear the regimes of bubble formation in complex entry flow within the ladle shroud, only one port gas injection was used in the present study, leaving gas flow rate and gas injection position as variables. The results of bubble measurements in each case are listed in Table I.

The initially released bubbles were formed under the shear action of high-speed liquid flow. Their sizes can be predicted by an empirical formula, proposed by Marshall.[12]

$$d_s = 0.96 R_{port}^{0.826} \left(\frac{u_{air}}{u}\right)^{0.36}, \quad [1]$$

where R_{port} represents the radius of the gas port, m; u is the velocity of the cross-flow, m/s; and u_{air} expresses the velocity of the air passing through the gas port, m/s, which can be calculated from the gas flow rate. Hence, the bubble size increased with the rising gas flow rate. This model was established, based on the assumption that bubbles are generated from a nozzle submerged in cross-flow liquid, without considering

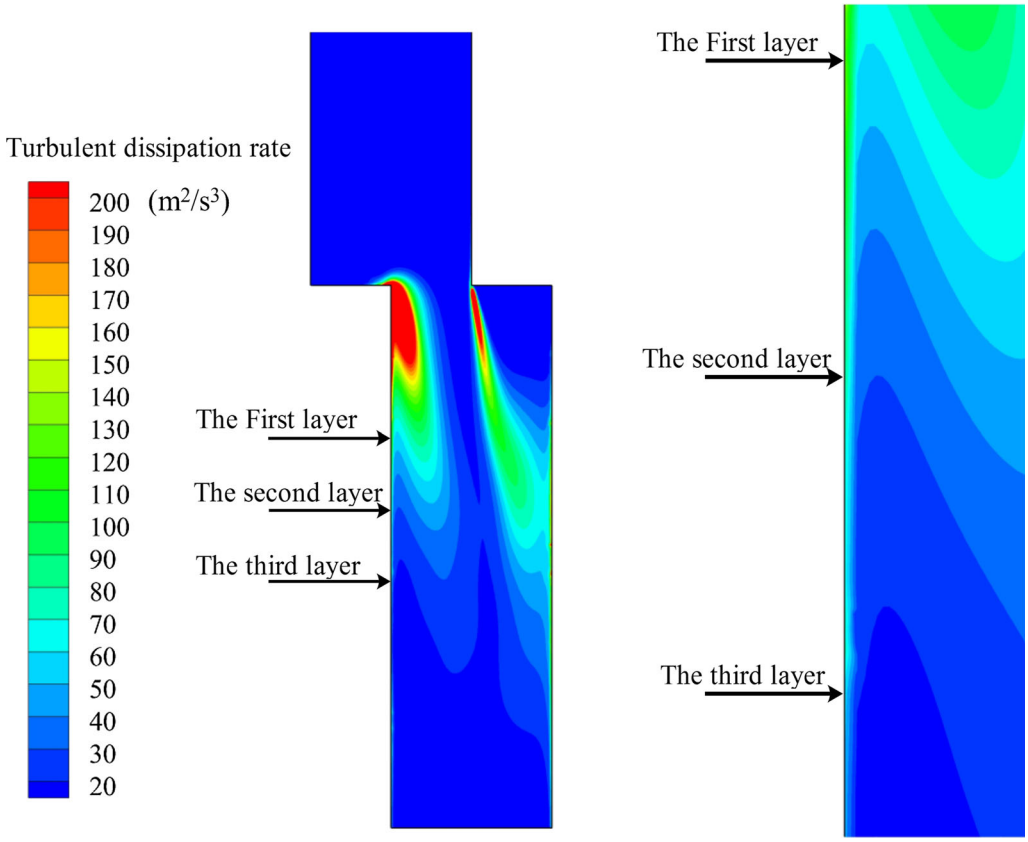

Fig. 4—Distribution of turbulence dissipation rate at the top part of the ladle shroud (reprinted from Ref. [11]).

the bubble break-up by turbulent flow, so that the bubble size predicted by Eq. [1], would be bigger than the result obtained in the present experiment.

The ladle shroud can be regarded as a mixing zone, due to the high turbulence kinetic energy of the entry flow within it. The bubbles in the shroud stream will be broken up once their Weber number exceeds a critical value, We_c. Evans *et al.*[13] carried out water experiments to produce bubbles under a wide range of gas injection parameters and flow conditions. A critical Weber number of 1.2 was determined by least square fitting, leading to a good agreement between model predictions and experimental data. Thus, the maximum size of bubbles within a violent turbulent flow can be given as

$$d_t = \left(\frac{We_c\sigma}{2}\right)^{3/5} \rho^{-3/5}\varepsilon^{-2/5}, \qquad [2]$$

where ρ is the density of liquid, kg/m^3; σ expresses the surface tension of liquid, N/m; and ε represents the turbulence dissipation rate, m^2/s^3.

The distribution of turbulent dissipation rate in the upper section of the ladle shroud was predicted by numerical simulation.[11] As shown in Figure 4, the bubble break-up by turbulent flow mainly occurs in the extent of 50 to 100 mm below the non-fully opened slide gate. The turbulence dissipation rate decreases along with the direction of entry flow. Therefore, the lowering of gas injection positions will weaken the effect of turbulence on bubble break-up, leading to bigger bubbles.

It is worth noting that, Eq. [2] was established based on the assumption that bubbles were indefinitely bathed in a turbulent flow with a uniform turbulence dissipation rate. Indeed, however, after departing from the gas port, bubbles were driven downward by the entry flow, and passed through the turbulent dissipation region in a limited time. Thus, bubbles cannot be thoroughly broken by turbulent flow.

As listed in Table II, the actual bubble size has an intermediate value between the predictions of the two models, under various operation parameters. As mentioned above, the formation of micro-bubbles can be regarded as a two-stage process, in the approach of gas injection into ladle shroud. On the basis of this theory, a semi-empirical model can be established to quantitatively analyze the size of bubbles under different operation conditions.

The size of bubbles initially formed by the cutting action of the liquid cross-flow is d_s as determined by Eq. [1]. The final size of the bubbles after turbulence refining will depend on the extent of the refining, *e.g.*, the time of bubbles bathing in the turbulent flow with a given turbulence dissipation level. If there is no further turbulence refining, the bubbles will keep their initial size d_s. With a sufficient turbulence refining, the final size of bubbles is d_t as determined by Eq. [2]. In practical flow systems, the turbulence dissipation rate is mostly

Table II. Comparison of Bubble Measurement and Model Predictions

Case	Turbulence Dissipation Rate (m^2/s^3)	Gas Flow Rate (L/min)	Bubble Measurement (μm)	Eq. [1] Prediction (μm)	Eq. [2] Prediction (μm)
1	90	0.1	675	1683	398
2	90	0.2	815	2160	398
3	90	0.4	965	2772	398
4	90	0.8	1117	3557	398
5	40	0.1	743	1683	550
6	40	0.2	895	2160	550
7	40	0.4	1132	2772	550
8	40	0.8	1380	3557	550
9	30	0.1	764	1683	617
10	30	0.2	915	2160	617
11	30	0.4	1287	2772	617
12	30	0.8	1664	3557	617

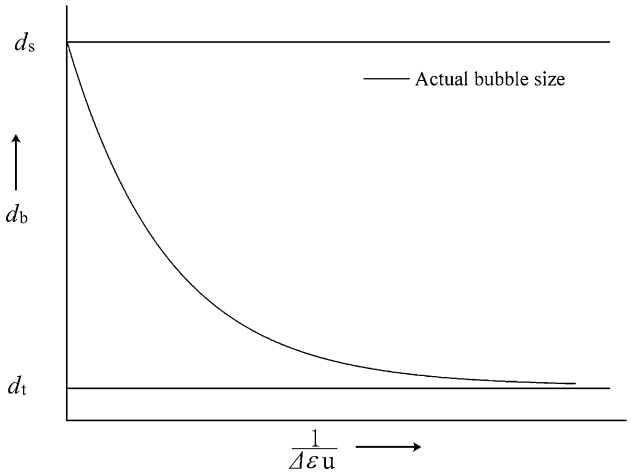

Fig. 5—Schematic illustration of bubble size evolution with turbulence refining extent.

non-uniform distributed and limited in a local region. Hence, the extent of bubble break-up by turbulence is also limited. Considering the incomplete break-up of bubbles by turbulence dissipation during the travel along a path of the decreasing turbulence dissipation, the bubbles may attain a stable characteristic size, between the initial bubble size, d_s and terminal size of bubble break-up, d_t.

Therefore, taking the exponential decreasing of bubble size with refining extent, the variation of final bubble size with refining extent can be schematically illustrated by Figure 5. This location depends on the traveling velocity and the gradient of the turbulence dissipation rate. For a given turbulence dissipation field, a greater traveling velocity leads to a shorter residence time for bubble break-up, so that the final size of bubble is bigger, being close to its initial size. Since the maximum turbulence dissipation rate in the region was already contained in d_s, turbulence dissipation rate gradient can be introduced to characterize the extent of bubble break-up. A higher turbulence dissipation rate gradient leads to a smaller region for bubble break-up, and thus a bigger bubble size under a given bubble velocity. Therefore, the reciprocal of $\Delta\varepsilon u$ can thus represent the extent of bubble refinement, as shown in Figure 5. The final bubbles size may be expressed as follows.

$$d_b = d_t + (d_s - d_t)e^{-\frac{C}{\Delta\varepsilon u}}, \quad [3]$$

where C is a model constant, –; $\Delta\varepsilon$ expresses the gradient turbulence dissipation rate, m/s^3; u represents the traveling velocity of bubbles within the ladle shroud, m/s.

It should be pointed out that Eq. [3] does not hold in the case of uniform turbulence dissipation or a bubble that is stationary, which is not expected to be encountered in practice. According to Eq. [3], in the limit of $\Delta\varepsilon u \to \infty$, the bubbles will have their initial size d_s, corresponding to zero extent of bubble refinement. In the limit of $\Delta\varepsilon u \to 0$, the bubbles will have the size d_t in equilibrium with ε, corresponding to maximum degree of bubble refinement.

The *Stokes* number shown by Eq. [4] can be used to assess the tracing accuracy of bubbles in a liquid flow field.[14]

$$Stk = \frac{\rho_g d_b u}{18\mu l_0}. \quad [4]$$

Here, ρ_g is the density of gas, kg/m^3; μ represents the dynamic viscosity of water, kg/(m s); and l_0 expresses the length scale associated with small vortices. As a result, the *Stokes* number is in the range of 0.0001 to 0.001 for the bubble size from 0.3 to 3 mm, indicating that all bubbles produced in this study can follow the liquid path line closely, with a tracking error less than 1 pct. Therefore, the bubbles' traveling velocity can be taken as the velocity of the entry flow.

In order to estimate the model constant, C, the least square method was used to achieve the fitting between the model and experimental data. The result indicates that a model constant (C) of 1929 gives the closest correlation to the experimental data. As shown in Figure 6, the model predictions are reasonably to the actual bubble sizes, with relative errors less than 16.8

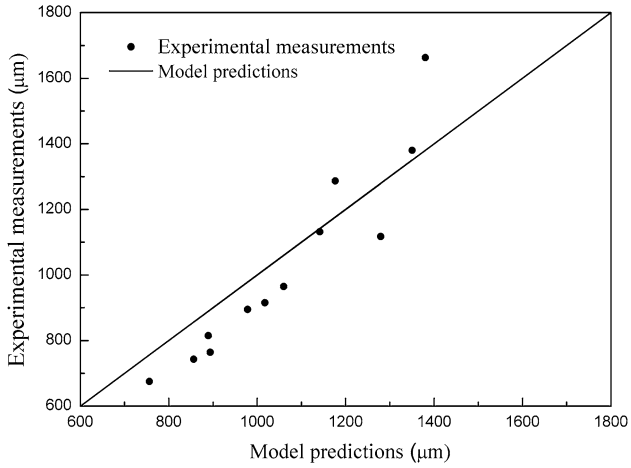

Fig. 6—Comparison between measured and predicted bubble sizes.

pct. Hence, this model is suitable to predict the size of bubbles formed by shearing flow coupled with strong turbulence.

In the present study, the formation of bubbles in a non-ideal flow was discussed, based on a full-scale water modeling. The shearing action on bubble departure and the non-fully bubble break-up by turbulence was considered. The following conclusions can be drawn from this study.

1. Gas injection into ladle shroud can effectively reduce the diameter of bubbles to micrometer scale. In this approach, the bubble formation was dominated by complex flow within the ladle shroud, which minimized the bubble growth caused by the poor wettability. Thus, this approach can produce bubbles less than 1mm in water modeling. It is expected this small bubble size can be replicated in actual tundish operations
2. The refining of bubbles is a two-stage process. Gas was initially separated from the orifice under the shearing action of high-velocity entry flow, forming primary bubbles; and then the bubble size is further refined by the turbulent flow within the ladle shroud. The effect of turbulence on bubble break-up depends on their traveling velocity and the dissipation rate of turbulence kinetic energy, and its gradient.
3. A semi-empirical model was developed to characterize the size of bubbles within a turbulent liquid flow of non-uniform turbulence dissipation. With a model constant (C) of 1929, the model prediction shows a good agreement with the experimental data, with relative errors smaller than 16.8 pct, over 12 cases with different gas injection operations.

The authors would like to appreciate Professor Roderick I.L. Guthrie and Dr. Mihaiela Isac, for providing all the research facilities in McGill Metals Processing Centre. We also acknowledge the financial support from NESRC and Nippon Steel & Sumitomo Metal Cooperation, for this work.

REFERENCES

1. K. Chattopadhyay, M. Hasan, M. Isac, and R.I.L. Guthrie: *Metall. Mater. Trans. B*, 2010, vol. 41B, pp. 225–33.
2. S. Chang, L.C. Zhong, and Z.S. Zou: *ISIJ Int.*, 2015, vol. 55, pp. 837–44.
3. A. Ramos-Banderas, R.D. Morales, L. Garcia-Demedices, and M. Diaz-Cruz: *ISIJ Int.*, 2003, vol. 43, pp. 653–62.
4. A. Cwudzinski: *Ironmak. Steelmak.*, 2010, vol. 37, pp. 169–80.
5. L.F. Zhang, J. Aoki, and B.G. Thomas: *Metall. Mater. Trans. B*, 2006, vol. 37B, pp. 361–79.
6. H.L. Yang, P. He, and Y.C. Zhai: *ISIJ Int.*, 2014, vol. 54, pp. 578–81.
7. L.F. Zhang and S. Taniguchi: *Int. Mater. Rev.*, 2000, vol. 45, pp. 59–82.
8. G.A. Irons and R.I.L. Guthrie: *Metall. Trans. B*, 1978, vol. 9B, pp. 101–10.
9. Z.Q. Liu, F.S. Qi, B.K. Li, and S.C.P. Cheung: *Int. J. Multiphase Flow*, 2016, vol. 79, pp. 190–21.
10. D. Mazumdar, G. Yamanoglu, R. Shankarnarayanan, and R.I.L. Guthrie: *Steel Res.*, 1995, vol. 66, pp. 14–19.
11. S. Chang, X.K. Cao, Z.S. Zou, M. Isac, and R.I.L. Guthrie: *Metall. Mater. Trans. B*, 2016, vol. 47B, pp. 2732–43.
12. S.H. Marshall, M.W. Chudacek, and D.F. Bagster: *Chem. Eng. Sci.*, 1993, vol. 48, pp. 2049–59.
13. G.M. Evans, G.J. Jameson, and B.W. Atkinson: *Chem. Eng. Sci.*, 1992, vol. 47, pp. 3265–72.
14. H.E.L. Haugen and S. Kragset: *J. Fluid Mech.*, 2010, vol. 661, pp. 239–61.